HHS Public Access

Author manuscript

Phys Chem Chem Phys. Author manuscript; available in PMC 2019 May 30.

Published in final edited form as:

Phys Chem Chem Phys. 2018 May 30; 20(21): 14927–14937. doi:10.1039/c8cp00352a.

Direct Observation of the Oxidation of DNA Bases by Phosphate Radical Formed under Radiation: A Model of Backbone-to-base Hole Transfer

MA Jun[a], **Jean-Louis Marignier**[a], **Pascal Pernot**[a], **Chantal Houée-Levin**[a], **Anil Kumar**[b], **Michael D. Sevilla**[b], **Amitava Adhikary**[b], and **Mehran Mostafavi**[a]

[a]Laboratoire de Chimie Physique, CNRS/Université Paris-Sud 11, Bâtiment 349, 91405 Orsay, France

[b]Department of Chemistry, 146 Library Drive, Oakland University, Rochester, Michigan 48309, USA

Abstract

In irradiated DNA, by base-to-base and backbone-to-base hole transfer processes, the hole (i.e., the unpaired spin) localizes on the most electropositive base, guanine. Phosphate radicals formed via ionization events in DNA-backbone must play an important role in the backbone-to-base hole transfer process. However, earlier works on irradiated hydrated DNA, on irradiated DNA-models in frozen aqueous solution and in neat dimethyl phosphate showed formation of carbon-centered radicals and not phosphate radicals. Therefore, to model backbone-to-base hole transfer process, we report picosecond pulse radiolysis studies of the reactions between $H_2PO_4^{\bullet}$ with DNA bases – G, A, T, and C in 6 M H_3PO_4 at 22 °C. The time-resolved observations show that in 6 M H_3PO_4, $H_2PO_4^{\bullet}$ causes one-electron oxidation of adenine, guanine and thymine, by forming the cation radicals via single electron transfer (SET) process; but, the rate constant of the reaction of $H_2PO_4^{\bullet}$ with cytosine is too low ($< 10^7$ L mol^{-1} s^{-1}) to be measured. The rates of these reactions are influenced by protonation states and reorganization energies of base radicals and of the phosphate radical in 6 M H_3PO_4.

Graphical Abstract

Correspondence to: Mehran Mostafavi.

Conflicts of interest

The authors declare there are no conflicts to declare.

Supporting Information (SI)

Supporting Information. Supporting information contains the following: (i) Normalized spectrum of guanine dissolved in aqueous solutions at different *pH*. (ii) UV-Visible absorption spectrum of guanine in fresh 6 mol L^{-1} H_3PO_4, of guanine in 6 mol L^{-1} H_3PO_4 recorded after 48 hours, of 6 mol L^{-1} H_3PO_4, and of glycine. The B3LYP-PCM/6-31++G** calculated optimized geometries of the complex of DNA base with $H_2PO_4^{\bullet}$. (iii) MCR-ALS analysis of adenine and thymine matrix data.

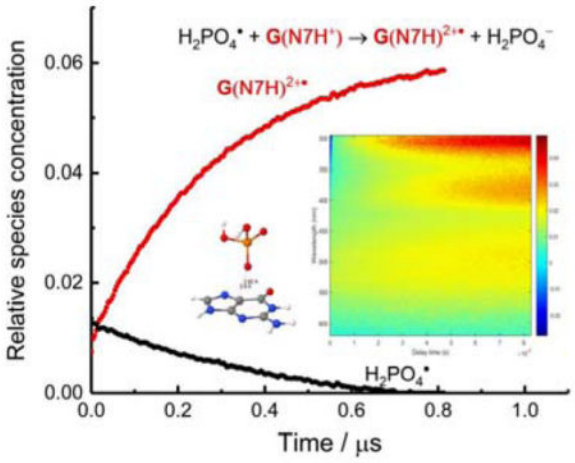

Introduction

The initial chemical events of cellular DNA damage exposed to ionizing radiation (γ- or X-ray photons, fast electrons, heavy ions, etc.) have been classified as: (i) indirect effect induced by the water-derived species, e.g., hydroxyl radical (•OH), water cation radical ($H_2O^{\bullet+}$), and low-energy electrons (LEEs), generated from energy deposited in the outer water shells surrounding the DNA. (ii) Direct-type effect that corresponds to the ionization and excitation of DNA components due to direct deposition of energy onto the DNA molecule. As a result of these excitations and ionization events occurring in the water molecules of first hydration layer, $H_2O^{\bullet+}$ and electrons are formed; $H_2O^{\bullet+}$ and the ejected electrons undergo both charge and spin transfer to the DNA (quasi-direct effect).[1–4] In addition, a considerable number of low energy electrons (LEE), are generated with excess kinetic energy of 0 to 20 eV, that damage DNA.[5,6]

The DNA backbone consists of alternating phosphate and sugar residues with high mass fraction (0.6). Therefore, on the basis of the number of valence electrons, the hydrated sugar-phosphate moiety can be significantly damaged either by the radiation-induced ionization-mediated one-electron oxidation events[7] or via indirect one-electron oxidation due to hole transfer from $H_2O^{\bullet+}$ formed in the hydration shell.[4]

Recent electron spin resonance (ESR) studies on radiation-mediated direct ionization of dimethyl phosphate and on γ-irradiated, as well as ion-beam irradiated, DNA showed that for sugar radical (*e.g.*, C5′•) formation, a very rapid ($< 10^{-12}$ s) deprotonation must occur from the one-electron oxidized sugar-phosphate backbone prior to the competitive backbone-to-base hole transfer.[4,7–10] Laser flash photolysis studies provided evidence that ionization of organic phosphates, such as ribose-5-phosphate, could produce the oxygen-centered primary phosphate radical, $O_3PO^{\bullet}$. Owing to the very oxidizing nature of $O_3PO^{\bullet}$, this radical undergoes fast intramolecular H-abstraction from the C4 of the pentoxyribose ring with rate constants up to $5 \times 10^7 s^{-1}$.[11] Therefore, if the lifetime of the hole in the sugar-phosphate backbone could be increased, the backbone-to-base hole transfer process could be directly probed using ESR spectroscopy. Via substitution of the phosphate by the easily

oxidizable phosphorothioate group at specific phosphate sites in the DNA backbone, this goal has been achieved.[8] The phosphorothioate-centered radicals have been shown to be formed in appreciable yields at the picosecond timescale, and subsequently lead to the fast one-electron oxidation of the proximate guanine base (i.e., backbone-to-base hole transfer) by temperature-activated hopping.

ESR spectroscopic studies did provide the evidence of phosphorus-centered radical by its large ^{31}P hyperfine couplings.[12,13] The phosphorous-centered radical was found to be produced in significantly reduced quantities at 77 K in hydrated (Γ(no. of water molecules per nucleotide) = 12) irradiated (temp. at irradiation = 77 K) DNA samples. These phosphorus-centered radicals were formed owing to the radiation-produced LEE-mediated fragmentation of the P-O bond in the sugar-phosphate backbone via the dissociative electron attachment (DEA) mechanism.[9]

From the viewpoint of backbone-to-base hole transfer and of carbon-centered sugar radical formation via the phosphate radical intermediate, it is therefore rationalized that reactivity of phosphate-centered radicals towards nucleobase sites would play an important role in radiation-induced DNA damage. However, apart from the work on S-oligomers, the role of phosphate radical in backbone-to-base hole transfer has not been sufficiently investigated to date. This might be due to the following reasons: (a) the LEE-mediated phosphorus-centered radical yield has been observed to be only about 0.1% of the total DNA-radicals present in ion-beam irradiated DNA;[4,7,13] (b) phosphate radicals are difficult to produce by radiation-induced reactive species, such as $^{\bullet}$OH. In fact, pulse radiolysis studies of the reaction of $^{\bullet}$OH with alkyl phosphates (a model of sugar-phosphate backbone) showed formation of only C-centered phosphatoalkyl radicals;[14] (c) a sufficient concentration of the phosphate radicals has to be achieved to carry out the investigation of the rate and the extent of the reaction between phosphate radicals and a nucleobase (i.e., backbone-to-base hole transfer).

The reasons (b) and (c) become particularly important in aqueous solutions under ambient conditions owing to various factors. First, the value of the rate constant of $^{\bullet}$OH with phosphate anions to form the phosphate radicals is found to be very low (~10^5 L mol^{-1} s^{-1})[15,16]; on the other hand, the reaction of $^{\bullet}$OH with the nucleobases being diffusion-controlled,[1,2] $^{\bullet}$OH predominantly reacts with the base moieties in DNA, in preference to the phosphates in the DNA-backbone. Secondly, in contrast to the formation of an oxidizing radical, *e.g.*, $SO_4^{\bullet-}$, via reaction of the radiation-produced electron with $K_2S_2O_8$, generation of phosphate radicals via electron addition to $K_2P_2O_8$ is not feasible. Moreover, photo-dissociation of peroxydiphosphate (e.g., $K_2P_2O_8$) in the presence of DNA-bases in aqueous solution at ambient temperature is not a suitable approach to study the reactions of phosphate radical with DNA-bases because $K_2P_2O_8$ being a very strong oxidant, would lead to the decomposition of the nucleobases during experiment.

To overcome the above-mentioned challenges and to observe the time-resolved reactivities of phosphate radicals with the individual DNA bases at room temperature, the present work introduces highly concentrated phosphoric acid (6 M) as a novel medium, based on our recent picosecond pulse radiolysis studies of direct and indirect effects of radiation.[17,18] In addition, our studies in highly concentrated phosphoric acid could better represent the

relevant molecularly crowded environments of localized hydrated DNA in nuclei than in dilute aqueous solutions. As an example, in concentrated phosphoric acid solutions (> 2 mol L^{-1}), the phosphate radical, $H_2PO_4^{\bullet}$, with an absorption maximum at 520 nm was clearly observed; its high radiolytic yield (~ 2×10^{-7} mol J^{-1}) is attributed to two ultrafast (within 7 ps electron pulse) parallel reaction pathways – (a) direct ionization of the phosphonate solutes, and, (b) electron transfer from water hole or water cation radical ($H_2O^{\bullet+}$) in close contact.[19] The lifetime of $H_2PO_4^{\bullet}$ is on the timescale of a few microsecond and its decay is mainly due to the reaction with $H^{\bullet}$.[19] In addition, the precursor of hydrated electron (pre-solvated electron), which is proposed to attack DNA molecules via dissociative attachment, is completely scavenged by H_3O^+ ions within the pulse (7 ps) when the concentration of H_3PO_4 is above 4 mol L^{-1}.[20] Meanwhile, the $H_2O^{\bullet+}$, precursor of $^{\bullet}OH$, is also partially quenched through electron transfer.[19] The side reactions stemming from pre-solvated electron and from solvated electron towards biomolecules, for example, nucleobases, are suppressed. Therefore, during the high-energy electron pulse radiolysis of 6 M phosphoric acid, the sufficient number of phosphoric groups produces optically detectable $H_2PO_4^{\bullet}$, and allows us to gain new insights of the rate and extent of one-electron oxidation of DNA bases - viz., thymine, guanine, adenine and cytosine, by $H_2PO_4^{\bullet}$ in aqueous solutions at ambient temperature. The rates of these reactions and the scaling of these rates can be accounted for by the extents of protonation of the DNA bases, as well as by the reorganization energies of the base radicals and $H_2PO_4^{\bullet}$ in 6 M H_3PO_4. These experimental studies, in combination with theoretical investigations, provide valuable insight on the backbone-to-base hole transfer process in irradiated DNA.

Materials and Methods

Compounds

The aqueous solutions were prepared using ultrapure water from an Elga system. The chemicals - guanine, thymine, cytosine, adenine, and phosphoric acid, were obtained from Sigma-Aldrich (purity > 99%) and were used as received (*i.e.*, without further purification). The solutions were saturated with oxygen (O_2, purity > 99.995% from Air Liquide) by bubbling before and during experiments. The solutions were irradiated at room temperature (21 ± 0.2°C).

Pulse radiolysis set-up

Pulse radiolysis experiments were carried out employing the picosecond laser-triggered electron accelerator, ELYSE, coupled with a time-resolved absorption spectrophotometric detection system.[21, 22] Electron pulses with 7.5 MeV energy, up to ~6 nC charge, and 15 ps duration were delivered at a repetition rate of 5 Hz. The sample was contained in a fused silica cell with a path length of 10 mm connected to a closed circulation system from a 150 mL Ar-purged stock solution used to renew the sample in the irradiation cell, after each pulse, by means of a peristaltic pump (flow rate 100 mL/min). The diameter of the electron beam was 3 mm, and the irradiated volume was less than 0.1 mL.

Absorption spectral measurements were performed using the original detection setup that we developed a few years ago. This setup is composed of a white light beam produced by a

homemade xenon flash lamp, focused through the sample collinearly with the electron beam, with a diameter smaller than the electron beam. It is then directed onto a flat field spectrograph (Chromex 250IS), which disperses the light on the entrance optics of a high dynamic range streak-camera (model C-7700-01 from Hamamatsu). This setup allows us to record the variation of the intensity of the analyzing light with a resolution time of 4 ps using the 500 ps to 1 ms sweep time/full scale in the wavelength range from 250 to 850 nm. Data are collected in the form of images with 1024 pixels on the time axis and 1344 pixels on the wavelength axis.

The flash lamp was synchronized with the electron pulse; as a result, an image resolved in wavelength and time was acquired. To improve the signal-to-noise ratio, series of 600 images were acquired and were then averaged in a single image used for the calculation of the absorbance by reference to the similar image obtained on the averaging of 400 flashes of the analyzing light without the electron pulse. The kinetic data and absorption spectra were both extracted from the same series of resulting images. In this work, the transient spectra were measured from 290 to 650 nm and from 40 ps to 10 μs.

Data analysis method

The data matrices images are analyzed by a multivariate curve resolution alternating least-squares (MCR-ALS) approach. The spectra of the absorbing species have been found to strongly overlap in this type of system; as a result, it becomes difficult to deconvolute individual spectra. Therefore, a global data analysis approach was used. Global matrices were built by delay-wise binding matrices for 6 M phosphoric acid with the data matrices for different time resolutions and concentrations. In this configuration, the individual spectra of various components are common to all of the experiments in the global data set, while each experiment has its own set of kinetic traces.

The number of distinguishable compounds in the global matrix was assessed by singular value decomposition (SVD). Subsequently, the MCR-ALS analysis with the corresponding number of species was performed. Positivity constraints were imposed for all spectra and kinetics. On the basis of quantum mechanical information, unimodality constraints can also be imposed to the spectra. Residuals maps were inspected to assess the absence of model inadequacy. All calculations have been made with codes developed in-house in the R environment. Our MCR-ALS code was adapted from the ALS package by K. M. Mullen.[23]

Theoretical Calculations

The geometries of $H_2PO_4^{\bullet}$ complexed with guanine (as a model of purine base) and cytosine (as a model of pyrimidine base) were fully optimized using the B3LYP/6-31++G** method as well as including the complete effect of aqueous solution via the integral equation formalism of the polarized continuum model (IEF-PCM) of Tomasi *et al.*[24,25] The complete methodology is herein designated as B3LYP-PCM/6-31++G**. All these calculations are performed employing the Gaussian 09 suite of programs (see supporting information).

Results and Discussion

High-energy electron pulse radiolytic measurements were performed in 6 M H_3PO_4 solutions in the presence of varying concentrations (0.25 to 20 mM) of DNA bases. The radiation-induced reactions taking place in these conditions are presented in Table 1. The solutions have been saturated by continuous O_2 bubbling for converting $H^\bullet$ to $HO_2^\bullet$ (R7); $HO_2^\bullet$ has been shown to be ineffective to nucleobases on the timescale of several microseconds.[3]

1. Phosphate radical ($H_2PO_4^\bullet$) formation in 6 M H_3PO_4 solution

In the absence of DNA base, the kinetics of formation and decay of phosphate radicals as a function of H_3PO_4 concentrations (3 to 14 M, Table 2) are compared in Figure 1. It is evident from Figure 1 that for a given absorbed dose per pulse, the initial absorbance slightly increases with the rise of H_3PO_4 concentration. The slow decay observed in 6–14 M phosphoric acid is mainly attributed to the reactions of phosphate radicals with $H^\bullet$ and $HO_2^\bullet$ (R10, R13, Table 1). At a relatively lower concentration of H_3PO_4 (3 M), the $^\bullet OH$ produced via proton transfer from $H_2O^{\bullet+}$ (R6) is not scavenged by H_3PO_4 and leads to the slight rise of phosphate radical via reactions R8 and R9. Aqueous H_3PO_4 at 6 M was selected as a "reference" medium for several reasons (Table 2). First, it constitutes a high solute electron fraction (*fs* = 0.43) environment in which direct ionization (R1) and hole transfer (R2) give rise to a significant yield (~1.5×10^{-7} mol J^{-1} at 100 ns) of $H_2PO_4^\bullet$.[19] The yield of this radical is larger than that of the remaining $OH^\bullet$ in the system. Secondly, the electrons either in their pre-hydrated or hydrated states are completely scavenged by H_3O^+ at tens of picoseconds (R3 and R4).[20] Thirdly, for 6 M H_3PO_4, plenty of water molecules are still available for biologically relevant reactions and are sufficient for dissolving the DNA bases.

In 6 M H_3PO_4 solution, the phosphate radical exists in its acidic form ($H_2PO_4^\bullet$). This conclusion is based on the fact that the transient spectrum showing the absorption maximum at 520 nm in the pulse radiolysis study of phosphoric acid (see Figure 1) matches to the one already reported and assigned to $H_2PO_4^\bullet$.[16,26] Previous studies by Katsumura *et al.*[16] provided an estimate of the standard potential of this radical as high as E^0 ($H_2PO_4^\bullet$, H^+/H_3PO_4) = 2.65 V (vs. NHE) on the basis of E^0 ($^\bullet OH$, H^+/H_2O) = 2.72 V. This standard potential value of $H_2PO_4^\bullet$ is as high as those of other strong one-electron oxidants, e.g., sulfate anion radical ($SO_4^{\bullet-}$), which has a standard potential of E^0 = 2.43 V vs. NHE.[27]

Concerning nucleobases, nucleosides and nucleotides, they are rapidly oxidized by sulfate anion radical ($SO_4^{\bullet-}$) with rate constants nearly at the diffusion-controlled limit.[27] The carbonate and dibromide anion radicals, $CO_3^{\bullet-}$ and $Br_2^{\bullet-}$, are weaker oxidants than $SO_4^{\bullet-}$;[3,28] $CO_3^{\bullet-}$ and $Br_2^{\bullet-}$ are known to oxidize guanine out of all four DNA bases.[28] Based on these observations, $H_2PO_4^\bullet$, which is a stronger oxidizing agent is predicted to be thermodynamically capable to cause the direct one-electron oxidation of all nucleobases ($E°$ from 2.03 to 2.5 eV) in aqueous solutions.

2. Guanine Oxidation by $H_2PO_4^{\bullet}$

Guanine has the lowest reduction standard potential among the four nucleobases (A, T, G and C). The holes (*i.e.*, unpaired spins) created by one-electron oxidation or by ionization events in irradiated DNA are eventually transferred to the guanine moiety, thereby producing transient guanyl radicals (guanine cation radical, $G^{\bullet+}$, or its neutral conjugate base, $(G(-H^{+})^{\bullet})$. Therefore, the structure and reactivity of these transient guanyl radicals, as the initial step in the oxidative damage of DNA, have been a center of interest ever since the early days of radiation chemistry and biology.[1–4, 29, 30] Guanine molecule is a derivative of purine; solubility of guanine in water is intrinsically low ($< 10^{-5}$ M), acting as the keto-9NH guanine tautomer moiety.[31] Three *pKa* values of guanine have been reported by experiments and by theoretical calculations as, 12.4, 9.4, and 3.3 corresponding to N9, N1, and N7, respectively.[32] In highly concentrated H_3PO_4 solutions (e.g., 6 M), the predominant species are monomer H_3PO_4 and dimer $H_5P_2O_8^-$ ions, as well as free H_3O^+ ion[33] (Table 2).

At such a low pH, our steady-state UV-visible spectral measurements show that the guanine molecule in phosphoric acid is in the fully protonated form and the complex, denoted ($G\cdots H_3PO_4$), is formed via H-bonding. In addition, the presence of phosphoric acid in water allows guanine to be dissolved in solution; furthermore, phosphoric acid does not cause degradation of guanine for at least over one week as found from UV-visible spectral studies. For the other three bases, concerns of their stability in concentrated H_3PO_4 solutions have been similarly examined and have been found to be similar to the above-mentioned results of guanine. More information on the chemical stability and structure of DNA bases in aqueous phosphoric acid are presented in SI (Figure SI1–Figure SI5).

In case of time-resolved spectroscopic measurements of H_3PO_4 in the presence of guanine induced by electron pulse, the evidence of reaction of $H_2PO_4^{\bullet}$ with guanine molecule giving rise to a new transient absorbing species is presented in Figure 2. Within the electron pulse (7 ps) the observed typical broad absorption spectrum with a maximum at 520 nm has suggested the immediate formation of $H_2PO_4^{\bullet}$ 0.1 μs after the pulse, the formation of additional radical(s) is evident from the appearance of three additional bands with one sharp peak located at 305 nm and two less intense ones - at 370 nm and 520 nm, respectively (see Figure 2, top and middle). The kinetics of formation of this intermediate is accelerated by increasing the guanine concentration (Figure 2, bottom). Moreover, the amount of radical observed at 300 nm increases by increasing guanine concentration, meaning that phosphate radical undergoes a number of competitive reactions (R10, R11 and R12 in competition with R16) and by increasing the guanine concentration, the oxidation reaction of guanine by phosphate radical is favored. Furthermore, the transient kinetics observed at 520 nm in which $H_2PO_4^{\bullet}$ has its maximal absorption, is found to differ much from those in the UV region (300 nm–375 nm) and is observed to level off over the 2 μs range (Figure 2, top).

The spectroscopic features of this transient species are in good agreement with that of the cation radical, $G^{+\bullet}$, formed after oxidation by $SO_4^{\bullet-}$ and $Br_2^{\bullet-}$ in aqueous solution by pulse radiolysis at room temperature, as well as by one-electron oxidation of the nucleoside dGuo in supercooled homogeneous solutions at low temperatures. [4,10,29,34,35] At neutral pH, it is well-accepted that the formation of $G^{+\bullet}$ in aqueous solutions is followed by a rapid deprotonation (1.8×10^7 s^{-1}) of the N1-H proton, i.e., the resulting radical is uncharged G

$(-H^+)^\bullet$. Optical and conductance studies at ambient temperature allowed estimation of the *pKa* value of $G^{+\bullet}$ of dGuo to be 3.9.[3,34] So, in basic medium, deprotonation of $G^{+\bullet}$ is characterized by a much pronounced change in the spectrum occurring at higher wavelength range ($\lambda > 600$ nm).[4,29] The rapid formation of $G(-H^+)^\bullet$ was also spectrophotometrically observed in single stranded and in duplex DNA by Kobayashi *et al.*[10(a)] In their work, absorbance at 650 nm which is referred to the typical electronic difference between $G^{+\bullet}$ and $G(-H^+)^\bullet$, is verified to be time-evolved and red-shifted. In 6 M H_3PO_4, guanine exists as N-7 protonated guanine as well as N-9 protonated guanine; upon one-electron oxidation, either the N-7 protonated or the N-9 protonated guanine cation radical ($G(N7H)^{2+\bullet}$ or $G(N9H)^{2+\bullet}$) undergo immediate deprotonation from N-7 or N-9 thereby forming the "pristine" $G^{+\bullet}$ (scheme 1 and vide supra).

From the existing literature, as well as under the highly acidic condition of our system (6 mol L^{-1} H_3PO_4), and based on our theoretical calculations, the *pKa* value of N7-protonated guanyl cation radical is predicted to be in the negative region.[36] Our results further establish that guanyl radical formed under highly acidic conditions of our system, exists predominantly in its cation radical state with the proton at N1 ($G^{+\bullet}$) instead of its N1-deprotonated state, $G(-H^+)^\bullet$ (vide infra).

As the spectra of various radical intermediates (e.g., $H_2PO_4^\bullet$, $G^{+\bullet}$) overlap with each other (e.g., see Figures 2 (Middle), 3 (Top)), MCR-ALS analyses have been performed subsequently to clarify the number of absorbing species and their corresponding spectra as well as their reaction pattern. Figure 3 (top) presents an example of the two-dimensional transient absorption spectra measured in 1 mmol L^{-1} guanine/6 mol L^{-1} H_3PO_4. Only two distinguishable transient absorbing species are sorted out by MCR-ALS analysis of the matrix spectral image. We have observed similarities of UV-Visible spectra in Figure 3 with those of the "pristine" $G^{+\bullet}$ that has already been reported in the literature.[29, 34 – 36] This can be explained by the rapid deprotonation of $G(N7H)^{2+\bullet}$ or $G(N9H)^{2+\bullet}$ already mentioned. None of the spectra in Figures 2 and 3 show any absorption peak of hydroxylated guanyl radicals that are formed due to addition of $^\bullet OH$ to guanine. For instance, the guanyl C4-OH adduct radical was characterized by a peak at 330 nm[37], and the guanyl C8-OH adduct radical should show a spectral feature at 610 nm.[38] Therefore, the remaining $^\bullet OH$, that is involved in the oxidation of G via addition-elimination process,[3,34,36–38] leads to the rapid formation of the same radical, $G^{+\bullet}$. The rate of this $^\bullet OH$-mediated formation of $G^{+\bullet}$ has to be faster than that the $G^{\bullet+}$ production via $H_2PO_4^\bullet$; $^\bullet OH$-mediated formation of $G^{\bullet+}$ is completed in less than 100 ns.[37] The correlated dynamic features of $G^{\bullet+}$ and $H_2PO_4^\bullet$ are presented in Figure 3 (bottom). The additional formation of $G^{+\bullet}$ after 100 ns is clearly observed by the faster kinetics; moreover, the rate of the $G^{+\bullet}$ formation is found accelerated by increasing the guanine concentration. On the other hand, the decay of $H_2PO_4^\bullet$ that is proportional to the increase of the $G^{+\bullet}$ confirms the direct one-electron oxidation of guanine by $H_2PO_4^\bullet$. It is worth noting that the cation radical, $G^{+\bullet}$ formed under our conditions, undergoes other processes - such as, hydration or solvation[4,30] at the several-microsecond timescale[39]. However, the transient spectrum that we obtain, show some distinct features when compared with previous reports of ($G^{+\bullet}$-H_2O) radicals (see supporting information Figure SI6 and SI7). Owing to the high concentration of phosphoric acid (6 M H_3PO_4) in our system, it is considered that phosphates may also compete with hydration process, giving rise to

phosphate adduct radicals at C8 of guanine. These and similar to •GOH-type radicals[30]. Benchmark UV-vis spectra of these radicals are not known albeit spectrum of •GOH has been reported [39]. In future, it is of great interest for us to address this issue.

Bimolecular rate constants (6.8×10^8 L mol^{-1} s^{-1}, Figure 4 and Table 3) were determined from the slopes of the linear plots of the observed pseudo-first-order rate constants against the guanine concentrations (Figure 4). It is worth noting here that one-electron reduction or H-atom abstraction of guanine by H• is not likely to take place in such acidic conditions. This is because the solutions employed here are O_2-saturated; as a result, H• is rapidly quenched by O_2 by producing $HO_2^•$ and the rate of reaction of $HO_2^•$ with G is not high enough to be competitive with that of $H_2PO_4^•$ with G.[3] One-electron oxidation of guanine by other radicals, such as $SO_4^{•-}$, was previously found to be nearly diffusion-controlled with a relatively higher rate (~3.2×10^9 L mol^{-1} s^{-1}).[35] The rate constant of oxidation of G in 6 M H_3PO_4 by $H_2PO_4^•$ is found to be lower in case of 6 M H_3PO_4 (see section 3 for discussion).

Our pulse radiolysis data (Figures 2–4) show that $H_2PO_4^•$ causes one-electron oxidation of DNA bases. To support the experimental observations, we have performed theoretical calculations on guanine (an example of purine base) for demonstrating the effect of $H_2PO_4^•$ on the oxidation of G and the effect of protonation of the G base on this oxidation. In the case of guanine, the C4=C5 double bond is well-known to add radicals, such as OH•, to form the G(C4-OH•) and G(C5-OH•) adducts.[25]

Based on this, we have investigated the addition of $H_2PO_4^•$ to the C4=C5 double bond of the guanine base moiety. Employing the B3LYP-PCM/6-31++G** method, the full (i.e., complete) geometry optimizations of G(C4-$H_2PO_4^•$) and G(C5-$H_2PO_4^•$) adducts show that $H_2PO_4^•$ does not form an adduct with either C4 or C5 of guanine. Rather, $H_2PO_4^•$ stabilizes itself over the plane of the guanine at distances between 2.8 Å to 3.0 Å, respectively (Figures 5(A) and 5(B)).

The spin density distributions of these conformations, calculated by B3LYP-PCM/6-31++G**, show that guanine is completely oxidized (spin density = 0.97 on guanine) to form $G^{+•}$ and $H_2PO_4^•$ is converted to its anion ($H_2PO_4^-$). Thus, electron transfer from guanine to $H_2PO_4^•$ (Figures 5(A) and 6(B)), is complete. Thus, the mechanism of reaction between G and $H_2PO_4^•$ is due to single electron transfer (SET). Since, in our system (6 M H_3PO_4), guanine is protonated at N7, we have checked whether this protonation can hinder the oxidation of guanine by $H_2PO_4^•$ via SET. Therefore, we fully optimized the geometries of N7-protonated guanine and the $H_2PO_4^•$ by employing B3LYP-PCM/6-31++G** method; the optimized structures ($N7H^+G$(C4-----$H_2PO_4^•$) and $N7H^+G$(C5-----$H_2PO_4^•$)) are shown in Figures 5(C) and 5(D). In this case, our calculations also predict that $H_2PO_4^•$ substantially oxidizes the protonated guanine and the spin density on N7 protonated guanine is found to be 0.63 for structure $N7H^+G$(C4-----$H_2PO_4^•$), (Figure 5(C)) and 0.72 for structure $N7H^+G$(C5-----$H_2PO_4^•$), (Figure 5(D)). Globally these results are in agreement with the oxidation of guanine by phosphate radical via SET. Thermodynamically, the reaction is favored at the C4–C5 site (Figure 5).

3. Adenine Oxidation and Thymine Oxidation/Addition by $H_2PO_4^{\bullet}$

Similar to our results found in guanine solutions, the observed absorbing radicals in adenine and thymine systems are assigned to be one-electron oxidized $[A(N1H)]^{2+\bullet}$ and $T^{+\bullet}$. The detailed experimental analyses and discussions are present in supporting information (Figures SI8 and SI9). The rate constant value of thymine case is surprisingly ca. 1.5 times higher than the corresponding one of guanine and is ca. 4 times higher than that of adenine under identical conditions (Figure 4). The high rate constant of T oxidation by $H_2PO_4^{\bullet}$ indicates that standard potential values of the DNA bases are not the only factor involved in the reaction between a DNA base and $H_2PO_4^{\bullet}$. Previous DFT calculations [40,41] suggested the protonation occurs preferentially at O4 in thymine, N3 in cytosine, N1 in adenine, and N7 in guanine. The proton affinity of thymine remains the lowest of all the nucleobases. The presence of acid (6 M H_3PO_4 in our case) may lead to increases of the standard potentials of DNA-base radical cation couples, E°(Base$^{+\bullet}$/Base), in varying degrees depending on the proton affinities of the bases. As a result, the one-electron oxidation rate of thymine case can be faster than those of other bases if it is not effectively protonated. In addition, this discrepancy can be attributed to possibly higher reorganization energies (for example, a Marcus-type effect) of base radicals and of $H_2PO_4^{\bullet}$ in 6 M H_3PO_4, compared to the reorganization energies of those (e.g., G(−H$^+$)$^{\bullet}$) in dilute aqueous solutions[42]. A small change in reorganization energy (e.g., 0.1 eV) can increase or decrease the rate constant of electron transfer reaction by one order of magnitude. Therefore, the different protonation states as well as reorganization energies of the base radicals and of $H_2PO_4^{\bullet}$ in 6 M H_3PO_4 would play a significant role in the electron transfer rates from the strongly protonated bases (G, A, C (for C, see section **4** below)) and the weakly protonated base (T) to $H_2PO_4^{\bullet}$.

In case of thymine, immediately after the formation of $T^{\bullet+}$, a pseudo-first-order decay of the cation radicals has been observed. This decay depends on the concentration of thymine (Figure SI9). On the basis of similar type of concentration-dependent decay of N-centered Hoechst 33258 radicals (N-centered H-258 radicals) which has been attributed to the aggregation of an N-centered H-258 radical with a parent H-258 molecule,[43] this concentration-dependent decay is attributed to the formation of thymine cation radical dimer ($T_2^{\bullet+}$). Moreover, following recent ESR studies,[42] $H_2PO_4^{\bullet}$ can add to the C5=C6 double bond of $T^{\bullet+}$ (see SI).

4. The Cytosine case

Figure 6 represents the transient spectra and kinetics of various amounts of cytosine in 6 M H_3PO_4 solutions. In our system (6 M H_3PO_4), cytosine might exist as the N3-protonated cytosine, (C(N3H$^+$)).[3,45] Owing to the increase of the ionization potentials of both protonated cytosine (C(N3H$^+$)) and protonated phosphate, $H_2PO_4^{\bullet}$,[40] it is expected that the rate of oxidation of C(N3H$^+$) by $H_2PO_4^{\bullet}$ should be lower than for G. It is evident from Figure 6 that the kinetics at 520 nm and 310 nm do not change significantly by varying cytosine concentration from as low as 0.25 mM to 20 mM. However, besides the absorption of $H_2PO_4^{\bullet}$ at 520 nm, we find a new absorption band at 425 nm whose intensity increases with the cytosine concentration. Our MCR-ALS analysis of 2D spectra (Figure 7) indicates that, compared to the three other DNA bases – G, A, and T - the decay of $H_2PO_4^{\bullet}$ in the presence of cytosine (0.25 mM to 20 mM) appears to be independent of cytosine

concentration. This finding suggests that $H_2PO_4^{\bullet}$ does not react or reacts very slowly (< 10^7 L mol^{-1} s^{-1}) with cytosine. Thus, the $H_2PO_4^{\bullet}$ induced cytosyl radical formation is not observed within tens of microsecond. However, formation of a new absorbing species has been observed at *ca*. 550 nm and it is correlated with cytosine concentration. This is due to the addition reaction of $OH^{\bullet}$ to cytosine either at C5 or at C6 of the C5=C6 double bond. [3, 45 – 47] The lifetime of this radical is estimated to be tens of microsecond. [3, 45 –47]

Again, similar to the guanine case, our theoretical calculations clearly present no evidence of $H_2PO_4^{\bullet}$ mediated adduct of cytosine; rather, only a complex with $H_2PO_4^{\bullet}$ stacked over cytosine is found (Figure 5E). The spin density distribution of this cytosine-$H_2PO_4^{\bullet}$ stacked system shows that 0.76 spin is localized on cytosine while 0.24 spin is localized on the H_2PO_4. Therefore, a possible oxidation of cytosine by $H_2PO_4^{\bullet}$ via SET cannot be ruled out; however, this reaction should be very slow. Thus, these results clearly show that the $H_2PO_4^{\bullet}$ mediated oxidation of pyrimidine nucleobases is kinetically controlled.

Conclusions

The salient features of the work reported here are the following:

1. *Implication of one-electron oxidation of DNA bases by $H_2PO_4^{\bullet}$ to the backbone-to-base hole transfer process in irradiated DNA:* the phosphate radical, $H_2PO_4^{\bullet}$, is an oxyl radical. Oxyl radicals are strong one-electron oxidizing radicals and can cause H-atom abstraction reaction. Analysis of our UV-visible pulse radiolysis spectra of DNA-base radical formed by the reactions of individual DNA base with $H_2PO_4^{\bullet}$ clearly presents the evidence of direct one-electron oxidation of G, A and T in 6 M H_3PO_4. However, the rate of oxidation of protonated cytosine by $H_2PO_4^{\bullet}$ is too slow to be detected by our system. These results, therefore, clearly indicate that the phosphate radical formed via direct ionization events in the sugar-phosphate backbone would oxidize the DNA bases; thus, these results should be treated as the benchmarks of backbone-to-base hole transfer process.

2. *The rate constants of the oxidation of a DNA base in acidic condition* (e.g., A, T, G, C) by $H_2PO_4^{\bullet}$ are with a decreasing order of T > G > A > C. These results point out that the formation of the DNA base cation radical (e.g., $G^{\bullet+}$) from the activated complex (e.g. $G(N7H^+)\cdots H_2PO_4^{\bullet}$) is much faster than the diffusion of reactants (i.e., $G(N7H^+)$, T or A and $H_2PO_4^{\bullet}$) and is mediated by SET. The values of the rate constant reported in Table 3 show clearly that the standard potential values of DNA bases [3, 45, 48] are not the only determining factors of oxidation reaction rate with $H_2PO_4^{\bullet}$. Considering Schemes 1, S1 and S2 and the different extents of protonation of the DNA-bases in 6 M H_3PO_4, with the proton affinity of T being the lowest [41], it is not surprising that the observed rate of one-electron oxidation of T by $H_2PO_4^{\bullet}$ is higher than those of the other bases. Also, the reorganization energies of protonated base radicals and of $H_2PO_4^{\bullet}$ in 6 M H_3PO_4 (Marcus-type effect) could be a factor in these SET reactions and in scaling the order of reactivity of these radicals towards the SET reactions. Also, the standard potentials of the radicals will be different in 6 M H_3PO_4.

3. *Nature of the DNA base radicals produced in our system (6 M H_3PO_4)*: It is evident from Schemes 1, S1 and S2 that the guanyl radical, produced by direct one-electron oxidation, is in its cation radical state. Adenyl radical is observed in its protonated cation radical state. Factors affecting reactivity of these radicals are discussed above (see point 2 (Conclusion) and section **3**, Results and Discussion).

The present study is limited to the fundamental model that shows the reactions between phosphate radicals and DNA bases in a highly concentrated medium (6 M H_3PO_4). In this work, we show that phosphate radicals undergo intermolecular reactions with nucleobases. However, taking into account the 3-dimentional model of charge transfer processes in DNA[49] and the proximity of the phosphate group to the base, the corresponding reaction in DNA is either intramolecular through-bond electron transfer, or intermolecular through-space electron transfer [49,50]. Therefore, the parameters that govern these two reactions (i.e., intermolecular and intramolecular) should be different. Nevertheless, our present work clearly demonstrates the direct observation of electron transfer from phosphate radical to the weakly protonated base DNA-base, thymine. It will be interesting, if possible, to extend investigation of the phosphate radical reactivity to the DNA-bases via an intramolecular reaction. Moreover, our earlier work[7] showed that the reaction of phosphate radicals in DNA either involves electron transfer from the sugar to the phosphate moiety followed by deprotonation, or alternatively, H-atom abstraction reactions by the phosphate radical from the 2′-deoxyribose moiety. Henceforth, we are extending our research efforts to study reactions of phosphate radicals with the DNA-models that are biologically relevant. Simultaneously, we are carrying out quantitative analyses to characterize stable molecular products that are formed via these reactions. These results will shed light into the mechanisms of this important oxidative pathway of DNA-damage.

Supplementary Material

Refer to Web version on PubMed Central for supplementary material.

Acknowledgments

MM thanks warmly to Prof. Kobayashi (Osaka University) for helpful discussions. AA, AK, and MDS acknowledge the National Cancer Institute of the National Institutes of Health (Grant RO1CA045424) for support. AA, AK, and MDS are also thankful to Research Excellence Fund (REF) and Center for Biomedical Research (CBR) at Oakland University for support.

References

1. O’Neill, P. Radiation-Induced Damage in DNA. In: Rao, BSM., Jonah, CD., editors. Radiation Chemistry: Present Status and Future Trends. Elsevier Science; Amsterdam: 2001. p. 585-622.
2. Mostafavi, Mehran, Douki, Thierry. Radiation Chemistry: From Basics to Applications in Material and Life Sciences. EDP Sciences; 2008.
3. von Sonntag, C. Free-radical-induced DNA Damage and Its Repair. Springer-Verlag; Berlin, Heidelberg: 2006. p. 213-482.
4. Adhikary, A., Becker, D., Sevilla, MD. Electron Spin Resonance of Radicals in Irradiated DNA. In: Lund, A., Shiotani, M., editors. Applications of EPR in Radiation Research. Springer International Publishing; Heidelberg, New York, London: 2014. p. 299-352.

5. Kumar, A., Sevilla, MD. Low Energy Electron (LEE) Induced DNA Damage: Theoretical Approaches to Modeling Experiment. In: Shukla, MK., Leszczynski, J., editors. Handbook of Computational Chemistry Volume III: Applications –Biomolecules. Springer-Verlag; Berlin, Heidelberg: 2012. p. 1215-1256.
6. Chen W, Chen S, Dong Y, Cloutier P, Zheng Y, Sanche L. Absolute Cross-sections for DNA Strand Breaks and Crosslinks Induced by Low Energy Electrons. Phys Chem Chem Phys. 2016; 18:32762–32771. [PubMed: 27878170]
7. Adhikary A, Becker D, Palmer BJ, Heizer AN, Sevilla MD. Direct formation of the C5′-radical in the sugar-phosphate backbone of DNA by high energy radiation. J Phys Chem B. 2012; 116:5900–5906. [PubMed: 22553971]
8. Adhikary A, Kumar A, Palmer BJ, Todd AD, Sevilla MD. Formation of S-Cl phosphorothioate adduct radicals in dsDNA-S-oligomers: Hole transfer to guanine vs. disulfide anion radical formation. J Am Chem Soc. 2013; 135:12827–12838. [PubMed: 23885974]
9. Zheng Y, Cloutier P, Hunting DJ, Sanche L, Wagner JR. Chemical basis of DNA sugar-phosphate cleavage by low-energy electrons. J Am Chem Soc. 2005; 127:16592–8. [PubMed: 16305248]
10. (a) Kobayashi K, Tagawa S. Direct Observation of Guanine Radical Cation Deprotonation in Duplex DNA Using Pulse Radiolysis. J Am Chem Soc. 2003; 125:10213–10218. [PubMed: 12926943] (b) Adhikary A, Khanduri D, Sevilla MD. Direct observation of the protonation state and hole localization site in DNA-oligomers. J Am Chem Soc. 2009; 131:8614–8619. [PubMed: 19469533]
11. Steenken S, Goldbergerova L. Photoionization of Organic Phosphates by 193 nm Laser Light in Aqueous Solution: Rapid Intramolecular H-Transfer to the Primarily Formed Phosphate Radical. A Model for Ionization-Induced Chain-Breakage in DNA? J Am Chem Soc. 1998; 120:3928–3934.
12. Celalyan-Berthier A, Berclaz T, Geoffroy M. Radiation damage in a phosphated sugar. An Electron Spin Resonance Study of Phosphorus-centered Radicals Trapped in an X-irradiated Single Crystal of a Phenoxyphosphoryl Xylofuranose Derivative. J Chem Soc Faraday Trans. 1987; 83:401–409.
13. Becker D, Adhikary A, Tetteh ST, Bull AW, Sevilla MD. Kr-86 ion-beam irradiation of hydrated DNA: Free radical and unaltered base yields. Radiat Res. 2012; 178:524– 537. [PubMed: 23106211]
14. Schuchmann MN, Scholes ML, Zegota H, von Sonntag C. Reaction of Hydroxyl Radicals with Alkyl Phosphates and the Oxidation of Phosphatoalkyl Radicals by Nitro Compounds. Int J Radiat Biol. 1995; 68:121– 131. [PubMed: 7658137]
15. Nakashima M, Hayon E. Rates of Reaction of Inorganic Phosphate Radicals in Solution. J Phys Chem. 1970; 74:3290–3291.
16. Jiang PY, Katsumura Y, Domae M, Ishikawa K, Nagaishi R, Ishigure K. Pulse Radiolysis Study of Concentrated Phosphoric Acid Solutions. J Chem Soc Fraday Trans. 1992; 88:3319–3322.
17. Ma J, Schmidhammer U, Pernot P, Mostafavi M. Reactivity of the Strongest Oxidizing Species in Aqueous Solutions: The Short-Lived Radical Cation $H_2O^{\bullet+}$ J Phys Chem Lett. 2014; 5:258–261. [PubMed: 26276210]
18. Ma J, LaVerne JA, Mostafavi M. Scavenging the Water Cation in Concentrated Acidic Solutions. J Phys Chem A. 2015; 119:10629–10636. [PubMed: 26449261]
19. Ma J, Schmidhammer U, Mostafavi M. Picosecond Pulse Radiolysis of Highly Concentrated Phosphoric Acid Solutions: Mechanism of Phosphate Radical Formation. J Phys Chem B. 2015; 119:7180–7185. [PubMed: 25176139]
20. Ma J, Schmidhammer U, Mostafavi M. Evidence for Transient Pair Formation between a Solvated Electron and H3O+ Observed by Picosecond Pulse Radiolysis. J Phys Chem Lett. 2014; 5:2219–2223. [PubMed: 26279537]
21. Belloni J, Monard H, Gobert F, Larbre JP, Demarque A, De Waele V, Lampre I, Marignier JL, Mostafavi M, Bourdon JC, et al. ELYSE A Picosecond Electron Accelerator for Pulse Radiolysis Research. Nucl Instrum Methods Phys Res Sect A. 2005; 539:527– 539.
22. Ma J, Wang F, Denisov SA, Adhikary A, Mostafavi M. Reactivity of Prehydrated Electrons towards Nucleobases and Nucleotides in Aqueous Solution. Sci Adv. 2017; 3:e1701669.doi: 10.1126/sciadv.1701669 [PubMed: 29250599]

23. Ruckebusch C, Sliwa M, Pernot P, de Juan A, Tauler R. Comprehensive data analysis of femtosecond transient absorption spectra: A review. J Photochem Photobiol C. 2012; 13:1–27.
24. Tomasi J, Mennucci B, Cammi R. Quantum Mechanical Continuum Solvation Models. Chem Rev. 2005; 105:2999–3094. [PubMed: 16092826]
25. Kumar A, Pottiboyina V, Sevilla MD. Hydroxyl Radical ($OH^{\bullet}$) Reaction with Guanine in an Aqueous Environment: A DFT Study. J Phys Chem B. 2011; 115:15129–15137. [PubMed: 22050033]
26. Maruthamuthu P, Neta P. Phosphate radicals. Spectra, Acid-base equilibriums, and Reactions with Inorganic Compounds. J Phys Chem B. 1978; 82:6–9.
27. Cadet J, Wagner JR, Shafirovich V, Geacintov NE. One-electron Oxidation Reactions of Purine and Pyrimidine Bases in Cellular DNA. Int J Radiat Biol. 2014; 90:423–432. [PubMed: 24369822]
28. Huie RE, Clifton CL, Neta P. Electron Transfer Reaction Rates and Equilibria of the Carbonate and Sulfate Radical Anions. Radiat Phys Chem. 1991; 38:477– 481.
29. Steenken S, Jovanovic SV. How Easily Oxidizable Is DNA? One-Electron Reduction Potentials of Adenosine and Guanosine Radicals in Aqueous Solution. J Am Chem Soc. 1997; 119:617–618.
30. Shukla LI, Adhikary A, Pazdro R, Becker D, Sevilla MD. Formation of 8-oxo-7,8-dihydroguanine-radicals in Gamma-irradiated DNA by Multiple One-electron Oxidations. Nucleic Acids Res. 2004; 32:6565– 6574. [PubMed: 15601999]
31. Bloomfield, VA., Crothers, DM., Tinoco, I, Jr. Physical Chemistry of Nucleic Acids. Harper & Row; New York: 1974.
32. Jing YH, Goddard WA III, Noyes KT, Sowers LC, Hwang S, Chung DS. pKa Values of Guanine in Water: Density Functional Theory Calculations Combined with Poisson−Boltzmann Continuum −Solvation Model. J Phys Chem B. 2003; 107:344–357.
33. Elmore KL, Hatfield JD, Dunn RL, Jones AD. Dissociation of Phosphoric Acid in Aqueous Solution at 25°C. J Phys Chem. 1965; 69:3520–3525.
34. Candeias LP, Steenken S. Structure and Acid-Base Properties of One-Electron-Oxidized Deoxyguanosine, Guanosine, and 1 –Methylguanosine. J Am Chem Soc. 1989; 111:1094– 1099.
35. O'Neill P, Davies SE. Pulse Radiolytic Study of the Interaction of $SO_4^{\bullet-}$ with Deoxynucleosides. Possible Implications for Direct Energy Deposition. Int J Radiat Biol. 1987; 52:577– 587.
36. Sevilla MD, Kumar A, Adhikary A. Comment on "Proton Transfer of Guanine Radical Cations Studied by Time-Resolved Resonance Raman Spectroscopy Combined with Pulse Radiolysis". J Phys Chem B. 2016; 120:2984– 2986. [PubMed: 26931377]
37. Phadatare SD, Sharma KKK, Rao BSM, Naumov S, Sharma GK. Spectral Characterization of Guanine C4-OH Adduct: A Radiation and Quantum Chemical Study. J Phys Chem B. 2011; 115:13650–13658. [PubMed: 22047605]
38. Candeias LP, Steenken S. Reaction of $HO^{\bullet}$ with Guanine Derivatives in Aqueous Solution: Formation of Two Different Redox Active OH-adduct Radicals and Their Unimolecular Transformation Reactions. Properties of G $(H)^{\bullet}$. Chem Eur J. 2000; 6:475– 484. [PubMed: 10747414]
39. Rokhlenko Y, Cadet J, Geacintov NE, Shafirovich V. Mechanistic aspects of hydration of guanine radical cations in DNA. J Am Chem Soc. 2014; 136:5956–62. [PubMed: 24689701]
40. Kumar A, Sevilla MD. Proton Transfer Induced SOMO-to-HOMO Level Switching in One-Electron Oxidized A:T and G:C Base Pairs: A Density Functional Theory Study. J Phys Chem B. 2014; 118:5453–5458. [PubMed: 24798145]
41. Russo N, Toscano M, Grand A, Jolibois F. Protonation of thymine, cytosine, adenine, and guanine DNA nucleic acid bases: Theoretical investigation into the framework of density functional theory. J Comput Chem. 1998; 19:989–1000.
42. Latus A, Alam MS, Mostafavi M, Marignier JL, Maisonhaute E. Guanosine radical reactivity explored by pulse radiolysis coupled with transient electrochemistry. Chem Commun. 2015; 51:9089– 9092.
43. Adhikary A, Bothe E, Jain V, von Sonntag C. Pulse radiolysis of the DNA-binding bisbenzimidazole derivatives Hoechst 33258 and 33342 in aqueous solutions. Int J Radiat Biol. 2000; 76:1157– 1166. [PubMed: 10993627]

44. Adhikary A, Kumar A, Heizer AN, Palmer BJ, Pottiboyina V, Liang Y, Wnuk SF, Sevilla MD. Hydroxyl Ion Addition to One-Electron Oxidized Thymine: Unimolecular Interconversion of C5 to C6 OH-Adducts. J Am Chem Soc. 2013; 135:3121– 3135. [PubMed: 23362972]

45. Steenken S. Purine bases, Nucleosides, and Nucleotides: Aqueous Solution Redox Chemistry and Transformation Reactions of Their Radical Cations and e- and OH adducts. Chem Rev. 1989; 89:503– 520.

46. Close DM. Calculated pKa's of the DNA Base Radical Ions. J Phys Chem A. 2013; 117:473– 480. [PubMed: 23282368]

47. Wagner JR, Cadet J. Oxidation Reactions of Cytosine DNA Components by Hydroxyl Radical and One-electron Oxidants in Aerated Aqueous Solutions. Acc Chem Res. 2010; 43:564– 571. [PubMed: 20078112]

48. Seidel CAM, Schulz A, Sauer MHM. Nucleobase-specific Quenching of Fluorescent Dyes. 1. Nucleobase One-electron Redox Potentials and Their Correlation with Static and Dynamic Quenching Efficiencies. J Phys Chem. 1996; 100:5541– 5553.

49. Cai, Z., Sevilla, MD. Studies of excess electron and hole transfers. In: Schuster, GB., editor. Long Range Charge Transfer in DNA II. Vol. 237. Springer; 2004. p. 103-127.Topics In Current Chemistry

50. Cukier E, Cave RJ. A comparison of through-space and through-bond coupling for tunneling in alkane chains. Chem Phys Lett. 2005; 402:186– 191.

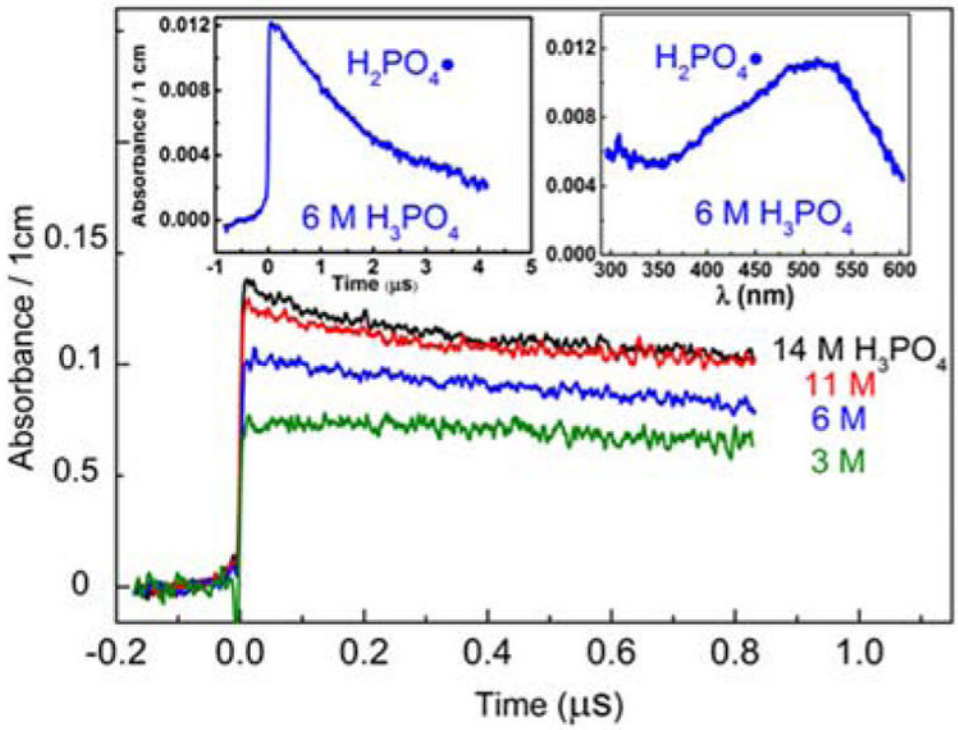

Figure 1.

Transient absorption spectra and kinetics measured in O_2-saturated aqueous phosphoric acid solutions. The radiation dose is 24 ± 0.5 Gy/pulse.

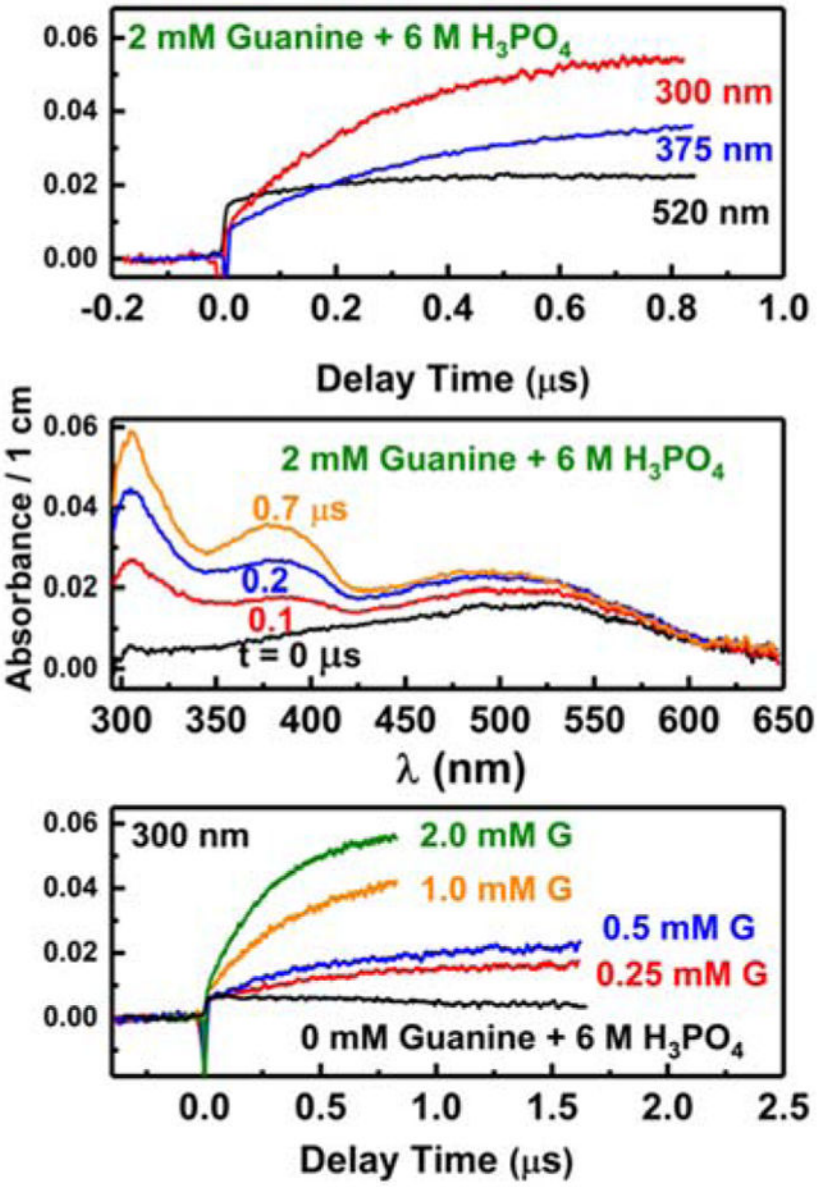

Figure 2.

Transient kinetic traces of 2 mM guanine/6 M H_3PO_4 observed at wavelengths of 300, 375 and 520 nm (top); Transient absorption spectra evolving with the delay time (middle); Transient kinetic trace at fixed wavelength of 300 nm for 6 M H_3PO_4 aqueous solutions dissolving guanine with concentration ranging from 0–2 mM (bottom).

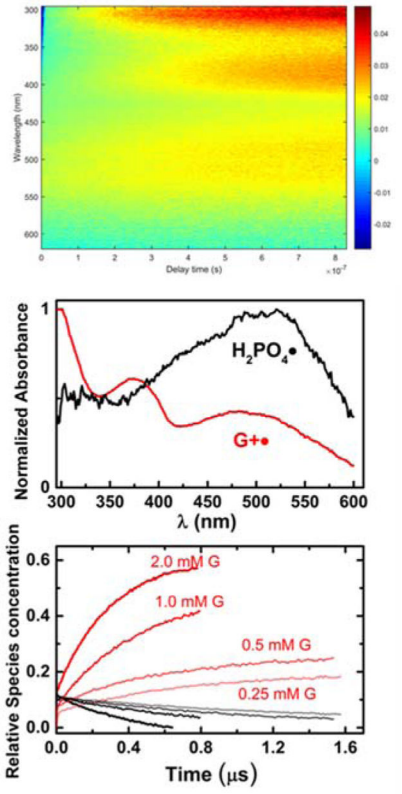

Figure 3.

Experimental two-dimensional image, showing the evolution of the absorbance at every wavelength versus time after one electron pulse applied in an aqueous 6 M H_3PO_4/1.0 mM guanine solution (top). The intensity profile of absorption spectra of absorbing species over the wavelength (middle) and kinetics of each species (bottom) result from the analysis via a MCR-ALS approach of above images recorded at different guanine concentrations.

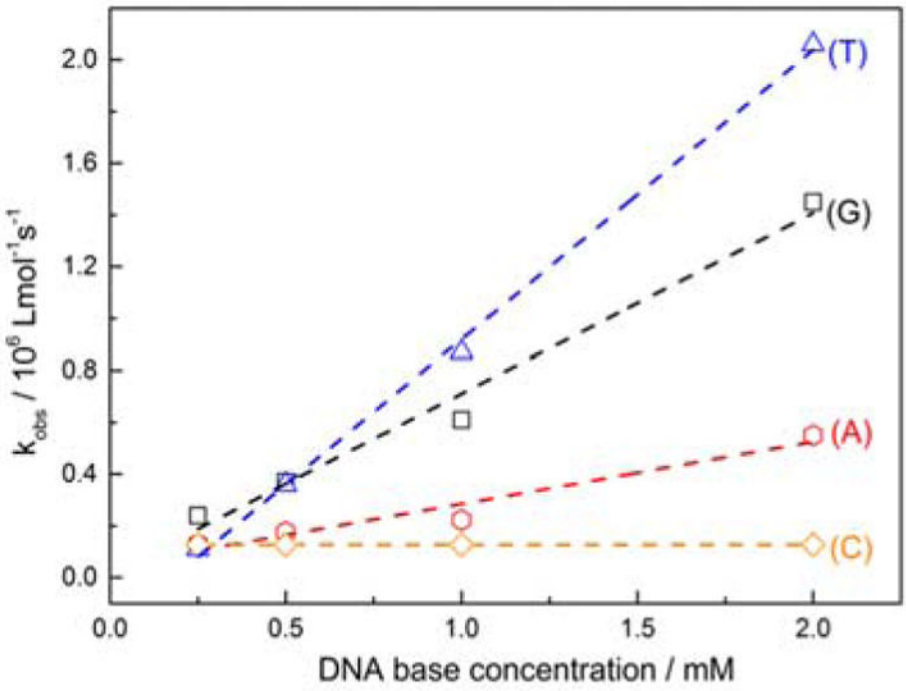

Figure 4.

Determination of the rate constant of oxidation of DNA bases oxidized by $H_2PO_4^{\bullet}$ from the pseudo-first order kinetics observed by varying the concentration.

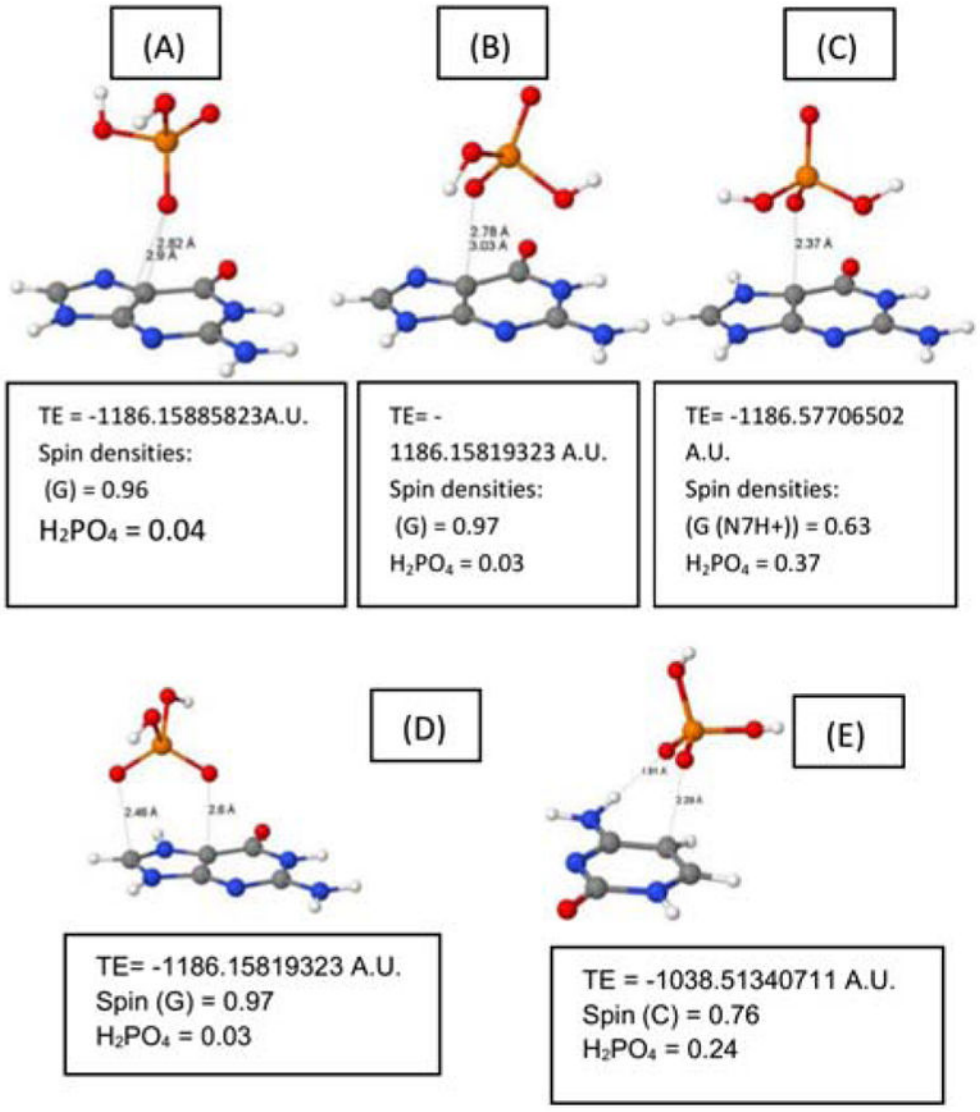

Figure 5.

Completely optimized geometries of $H_2PO_4^{\bullet}$ that is proximate to and over guanine C4=C5 double bond: G (C4-----$H_2PO_4^{\bullet}$) (A) and G (C5-----$H_2PO_4^{\bullet}$) (B). Completely optimized geometries of the complexes of $H_2PO_4^{\bullet}$ that is proximate to and over N7-protonated guanine C4=C5 double bond: $N7H^+G$ (C4-----$H_2PO_4^{\bullet}$) (C) and $N7H^+G$ (C5-----$H_2PO_4^{\bullet}$) (D). Optimized geometry of $H_2PO_4^{\bullet}$ that is proximate to and over N3-protonated cytosine C5=C6 double bond. The geometries were optimized employing B3LYP-PCM/6-31++G** method, the total energy (TE) and the spin density distributions on $H_2PO_4^{\bullet}$ as well as on DNA-base moiety are indicated.

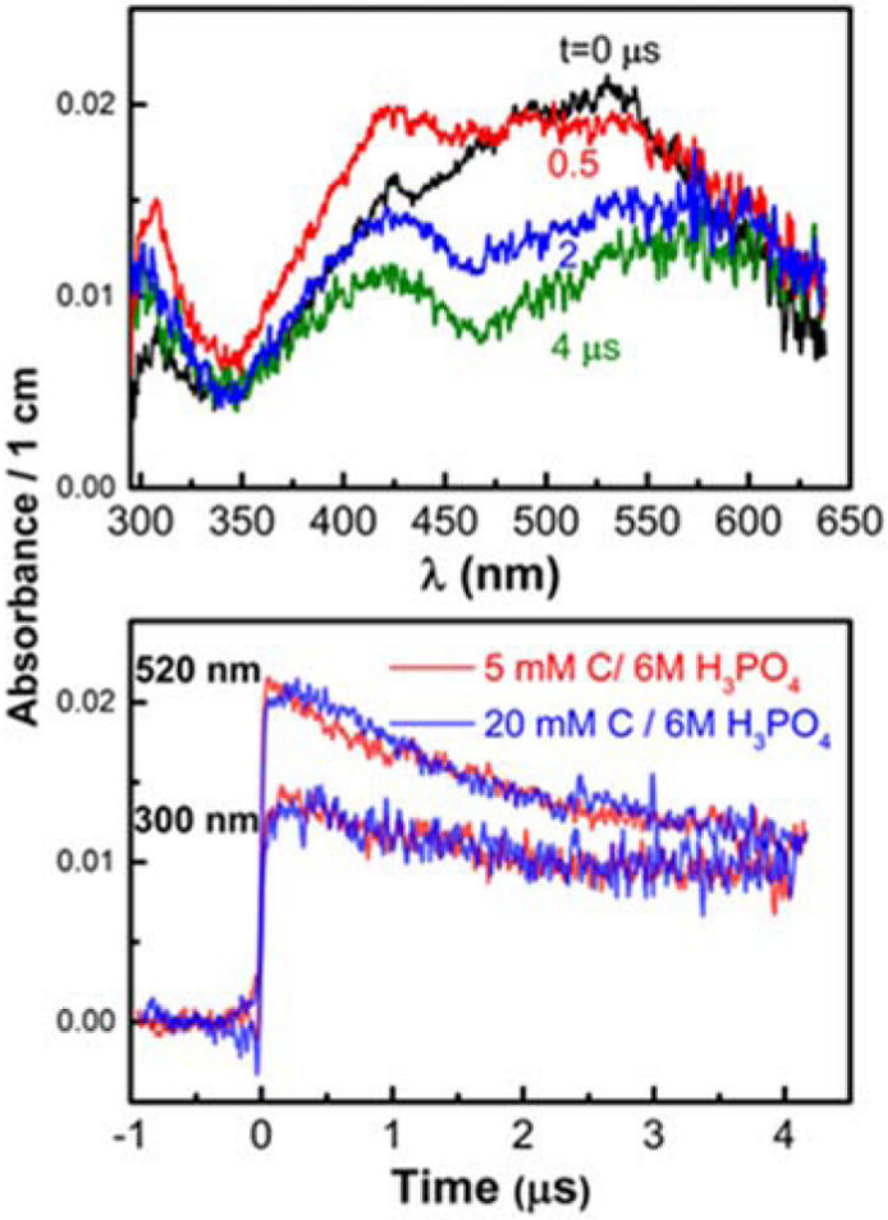

Figure 6.

Transient absorption spectra evolving with the delay time (up); Transient kinetic trace at fixed wavelength of 310 nm and 520 nm for 6 M H_3PO_4 aqueous solutions dissolving cytosine with concentrations ranging from 5 mM up to 20 mM (bottom).

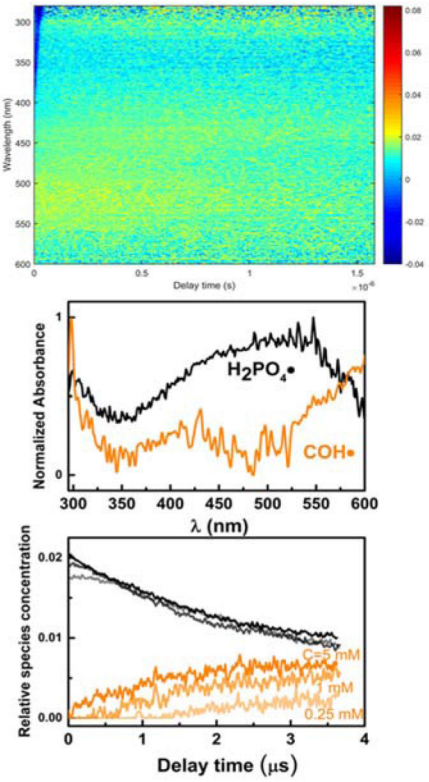

Figure 7.

Experimental two-dimensional image, showing the evolution of the absorbance at every wavelength versus time after one electron pulse applied in an aqueous 6 M H_3PO_4/1.0 mM cytosine solution (top). The intensity profile of absorption spectra of absorbing species over the wavelength (middle) and kinetics of each species (bottom) result from the analysis via a MCR-ALS approach of above images recorded at different cytosine concentration.

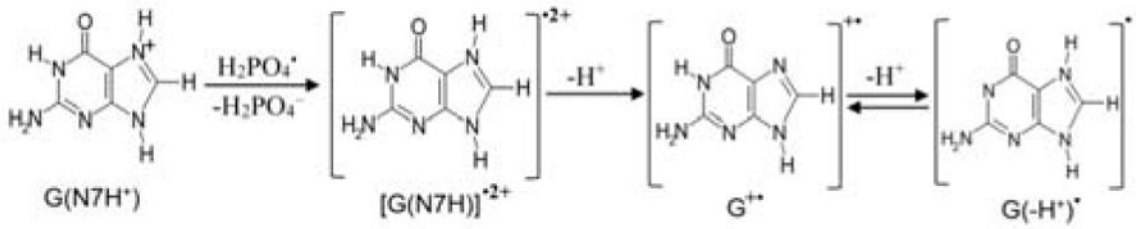

Scheme 1.

Formation of $G^{+\bullet}$ via one-electron oxidation of $G(N7H^{+})$ by $H_2PO_4^{\bullet}$ followed by deprotonation of $G(N7H)^{2+\bullet}$ in 6 M H_3PO_4. In neutral media, The conversion of $G^{+\bullet}$ to its conjugate base, $G(-H^{+})^{\bullet}$ in neutral solution,[3,4,10] is also shown.

Table 1

Reaction scheme for the oxidation of DNA bases via ionizing radiation in highly concentrated phosphoric acid solutions. k and τ represent the reaction rate constants and reaction times, respectively.

	Reaction	$k(M^{-1}s^{-1})$ or τ (s)
R1	H_3PO_4, $H_2PO_4^-$, HPO_4^{2-}, $PO_4^{3-} \rightarrow H_3PO_4^{+\bullet}$, $H_2PO_4^\bullet$, $HPO_4^{\bullet-}$, $PO_4^{\bullet 2-} + e^-$	$< 10^{-13}$ s [ref18]
R2	H_3PO_4, $H_2PO_4^-$, HPO_4^{2-}, $PO_4^{3-} + H_2O^{\bullet+} \rightarrow H_3PO_4^{+\bullet}$, $H_2PO_4^\bullet$, $HPO_4^{\bullet-}$, $PO_4^{\bullet 2-} + H_2O$	$< 10^{-13}$ s [ref18]
R3	$e^- \rightarrow e_{hyd}^-$	$< 10^{-12}$ s [ref 20]
R4	$e^- + H_3O^+ \rightarrow H^\bullet + H_2O$	$< 10^{-12}$ s [ref 20]
R5	$e_{hyd}^- + H_3O^+ \rightarrow H^\bullet + H_2O$	2.3×10^{10} [ref 20]
R6	$H_2O + H_2O^{\bullet+} \rightarrow H_3O^+ + OH^\bullet$	$< 10^{-13}$s [ref 18]
R7	$H^\bullet + O_2 \rightarrow HO_2^\bullet$	2.1×10^{10} [ref 16]
R8	$OH^\bullet + H_3PO_4 \rightarrow H_2PO_4^\bullet + H_2O$	4.2×10^4 [ref 16]
R9	$OH^\bullet + H_2PO_4^- \rightarrow HPO_4^{\bullet-} + H_2O$	2.0×10^4 [ref 16]
R10	$H_2PO_4^\bullet + H^\bullet \rightarrow H_3PO_4$	1.3×10^{10} [ref 16]
R11	$H_2PO_4^\bullet + H_2PO_4^\bullet \rightarrow H_4P_2O_8$	2.5×10^9 [ref 16]
R12	$H_2PO_4^\bullet + OH^\bullet \rightarrow H_3PO_5$	4.0×10^9 [ref 16]
R13	$H_2PO_4^\bullet + HO_2^\bullet \rightarrow H_3PO_4 + O_2$	3.0×10^9 [ref 16]
R14	$H_2PO_4^\bullet + H_2O_2 \rightarrow H_3PO_4 + HO_2^\bullet$	3.5×10^9 [ref 16]
R15	$OH^\bullet$+ Bases $\rightarrow$ Bases-$OH^\bullet$ or $Bases^{+\bullet} + OH^-$	see text
R16	$H_2PO_4^\bullet$+ Bases $\rightarrow$ $Bases^{+\bullet} + H_2PO_4^-$	see text

Table 2

Chemical composition of phosphoric acid solutions at different concentrations.

C [mol L^{-1}]	H^+	$H_2PO_4^-$	$H_5P_2O_8^-$	H_3PO_4	$H_6P_2O_8$	$[H_2O]/[H_3PO_4]$	$[H_2O]/P$
2	0.353	0.0912	0.262	1.22	0.0844	25.3	30.53
4	0.904	0.0987	0.805	1.64	0.3238	11.2	15.62
6	1.696	0.09	1.606	1.45	0.6245	6.5	10.34
8	2.695	0.0742	2.620	0.99	0.8463	4.2	7.42
11	4.182	.0539	4.326	0.56	1.067	2.4	4.4
13	5.096	0.038	5.058	0.385	1.23	1.46	2.83
14.6	5.733	0.0297	5.70	0.320	1.475	0.96	1.88

Table 3

Rate constants for reactions of $^{\bullet}OH$ and $SO_4^{\bullet-}$ with various DNA bases at pH~7. Rate constants of reactions of $H_2PO_4^{\bullet}$ with nucleobases including their oxidation in 6 M H_3PO_4 are reported in the present work. Standard redox potentials of nucleotide base cation radicals are also mentioned.

DNA bases	$k(OH^{\bullet})$[43,45] L $mol^{-1}s^{-1}$	$k(SO_4^{\bullet-})$[35] L $mol^{-1}s^{-1}$	$k(H_2PO_4^{\bullet})$ L mol^{-1} s^{-1}	E° ($dB^{\bullet+}$/dB) vs. NHE[48]
(G)	9.2×10^9	~4.1×10^9	6.9×10^8	1.47 V
(A)	6.1×10^9	4.6×10^9	2.4×10^8	1.94 V
(T)	7.4×10^9	~2.1×10^9	1.1×10^9	2.09 V
(C)	6.3×10^9	~1.6×10^9	$< 5\times 10^7$	2.12 V